K-SPACE MOSAICKING BY COHERENTLY COMBINING SINGLE-PASS MONOSTATIC AND BISTATIC SAR IMAGES

Ingo Walterscheid, Andreas R. Brenner

Fraunhofer Institute for High Frequency Physics and Radar Techniques FHR,
Neuenahrer Str. 20, 53343 Wachtberg, Germany
Email: ingo.walterscheid@fhr.fraunhofer.de

1. INTRODUCTION

The $\mathbf{k}$-space as the domain of the spatial Fourier transform presents an important mathematical tool for general imaging problems [1]. In the field of radar imaging, the $\mathbf{k}$-space can serve as a system analysis tool as well as the basis for reconstruction algorithms. Furthermore, the $\mathbf{k}$-space can be very helpful to design and optimize the flight paths in a bi- or multistatic configuration for a specific application.

Using a classical monostatic SAR the shape of the set $\mathbf{K}$, which comprises all possible wavenumber vectors $\mathbf{k}(T)$ during data acquisition, turns out to be a section of a circular ring. The extent of the set $\mathbf{K}$ is determind by the signal bandwidth and the aspect angle variation. Using a bistatic SAR with two transmit and receive sensors we get three $\mathbf{k}$-sets which can be coherently combined to get a larger contiguous $\mathbf{k}$-set as a base for a resolution improved SAR image. Although the analysis of an incoherent combination of the $\mathbf{k}$-sets would be very interesting, the paper concentrates on the coherent combination of the individual $\mathbf{k}$-sets of across-track and along-track bistatic data acquisitions. A big advantage is that the two monostatic and the bistatic data sets are acquired simultaneously, which prevents a decorrelation of the data.

2. GEOMETRY AND K-SPACE

2.1. Three dimensional geometry

If we look at the general three-dimensional situation in a cartesian coordinate system as sketched in Fig. 1, one sensor is placed at the position $\mathbf{R}_1 = (x, y, z)^t$ and the other sensor at $\mathbf{R}_2 = (x, y, z)^t$. A point target is located at $\mathbf{r} = (x, y, z)^t$. The angle between the two sensors with the vertex at the target is the bistatic angle β. The bistatic range R is defined as the sum of the individual ranges R_1 and R_2

$$R(T;\mathbf{r}) = R_1(T;\mathbf{r}) + R_2(T;\mathbf{r}) = |\mathbf{r} - \mathbf{R}_1(T)| + |\mathbf{r} - \mathbf{R}_2(T)|, \tag{1}$$

with T the slow time parameter. The unit vectors $\mathbf{u}_i(T;\mathbf{r})$ are defined as

$$\mathbf{u}_i(T;\mathbf{r}) = \frac{\mathbf{r} - \mathbf{R}_i(T)}{|\mathbf{r} - \mathbf{R}_i(T)|}, \qquad i = 1, 2 \tag{2}$$

and look from the sensors to the point target. We also define an effective direction vector

$$\mathbf{u}_{\mathit{eff}}(T;\mathbf{r}) = \frac{1}{2}\big(\mathbf{u}_1(T;\mathbf{r}) + \mathbf{u}_2(T;\mathbf{r})\big), \tag{3}$$

which points in the direction of the bisector of the bistatic angle. Note that the length of this vector can be much lower than 1 depending on the bistatic angle β. The length of $\mathbf{u}_{\mathit{eff}}$ is given by $\cos(\beta/2)$.

The individual wavenumber vectors are given by

$$\mathbf{k}_i(T;\mathbf{r}) = k\,\mathbf{u}_i(T;\mathbf{r}), \qquad i = 1, 2, \tag{4}$$

with $k = 2\pi/\lambda$ and λ the wavelegth. The effective wavenumber vector $\mathbf{k}_{\mathit{eff}}$ is given by

$$\mathbf{k}_{\mathit{eff}}(T;\mathbf{r}) = \frac{1}{2}\left(\mathbf{k}_1(T;\mathbf{r}) + \mathbf{k}_2(T;\mathbf{r})\right) = k\,\mathbf{u}_{\mathit{eff}}(T;\mathbf{r}). \tag{5}$$

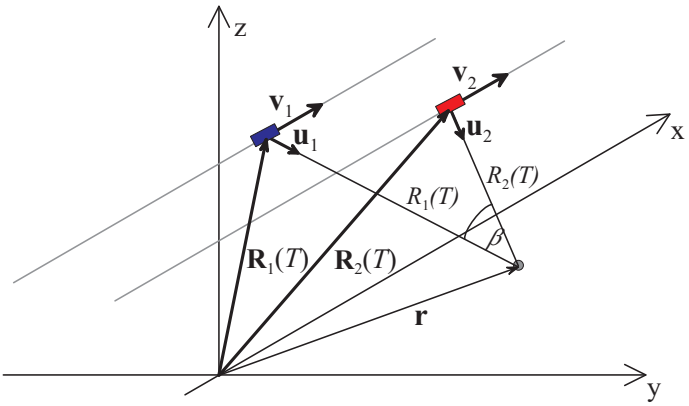

Fig. 1. Geometry of a bistatic across-track configuration.

2.2. Defining of monostatic and bistatic k-sets

Generally, the scene to be imaged can be described as a three dimensional complex reflectivity distribution a($\mathbf{r}$). Its 3D-Fourier transform A($\mathbf{k}$) is a complex function of the wavenumber vector $\mathbf{k}$. The domain of these vectors is called the $\mathbf{k}$-space [1]. The monostatic SAR data acquisition corresponds to a certain $\mathbf{k}$-set $\mathbf{K}_i$ which can be described by

$$\mathbf{K}_i := \{k\,\mathbf{u}_i(T) : k \in [k_1, k_2],\, T \in [T_1, T_2]\}, \qquad i = 1, 2. \tag{6}$$

In the bistatic case, the $\mathbf{k}$-set is given by [2]

$$\mathbf{K}_{bi} := \{k\,\mathbf{u}_{\mathit{eff}}(T) : k \in [k_1, k_2],\, T \in [T_1, T_2]\}. \tag{7}$$

3. BISTATIC ALONG-TRACK CONFIGURATION

Using a bistatic along-track configurtion, where transmitter and receicver fly along the same track with the same velocity, the azimuth resolution can be increased by the coherent combination of the shifted spectrums due to different Doppler centroids. Furthermore, even the range resolution can be increased by the combination of the monostatic and bistatic $\mathbf{k}$-sets. Due to the fact that the effective direction vecotor $\mathbf{u}_{\mathit{eff}}$ depends on the bistatic angle and can be much lower than 1, the radial position and extent of the bistatic $\mathbf{k}$-set is different to the monostatic one. Therefore, the radial extent of the complete $\mathbf{k}$-set can be larger than that of the individual $\mathbf{k}$-sets.

4. BISTATIC ACROSS-TRACK CONFIGURATION

The slant range resolution of a synthetic aperture radar is limited by the signal bandwidth of the transmitted waveform. The reduced corresponding geometric resolution on ground depends on the incidence angle. In the past, it was shown that the geometric resolution can be improved by coherent combination of multiple SAR images acquired with slightly different incidence angles [3, 4, 5]. A big drawback of this repeat-pass acquisition is that parts of the scene can change during the subsequent data collections including decorrelation. The strength of decorrelation depends on the scene content itself, the revisit period, which can be e. g. multiple hours for spaceborne sensors and the used frequency band.

Using two sensors in an across-track configuration, two monostatic and a bistatic image can be simultaneously acquired and after their coherent combination the ground range resolution can be improved significantly without any problems due to temporal decorrelation. Even in the case that there is no overlap between the two monostatic ground projected $\mathbf{k}$-sets, it is quite possible that the ground projected $\mathbf{k}$-set of the bistatic data coincide with the first as well as with the second monostatic $\mathbf{k}$-set, resulting in a larger contiguous $\mathbf{k}$-set as a base for a resolution improved SAR image.

Figure 2 sketches the monostatic and bistatic $\mathbf{k}$-sets and the corresponding ground projected $\mathbf{k}$-sets in the y-z-plane. The two sensors move in x-direction into the y-z-plane. A point target in the origin is illuminated by sensor 1 with the incidence angle ψ_1 and by the sensor 2 with the incidence angle ψ_2. Due to the fact, that there is no overlap between the projected monostatic $\mathbf{k}$-sets a combination and resolution enhancement is not possible. Using additionally the bistatic $\mathbf{k}$-set (green) the gap can be bridged, resulting in a large contiguous $\mathbf{k}$-set $\mathbf{K}_c$ in the ground plane.

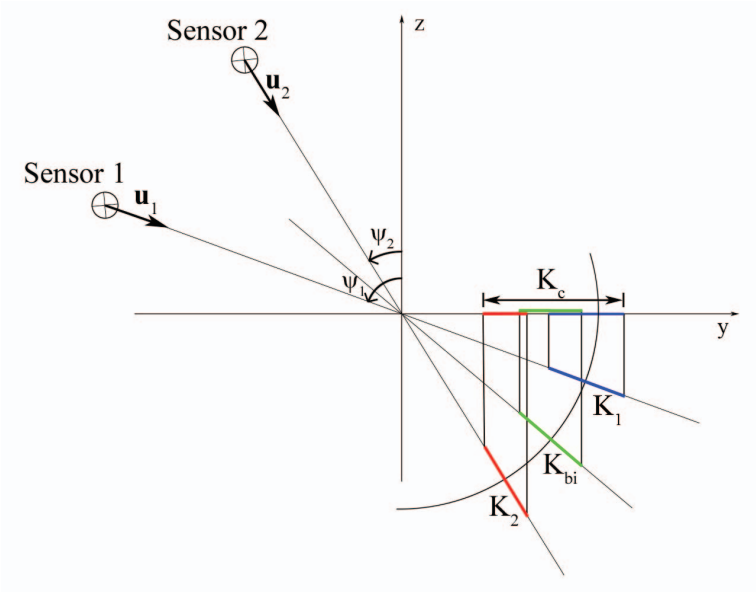

Fig. 2. Monostatic and bistatic k-sets in the y-z-plane and the corresponding projections on ground.

5. EXPERIMENTS USING MULTIPLE MONOSTATIC REPEAT-PASS SAR IMAGES

Due to an actual lack of appropriate simultaneously acquired monostatic and bistatic data, three monostatic data sets of a scene acquired with different incidence angles will be used to show the potential of combining k-sets with respect to resolution enhancement. The data have been acquired with the airborne X-band SAR system PAMIR [6]. The temporal decorrelation was minimized by operating a very short revisit period of about 6 minutes. The three data sets have been acquired with a signal bandwidth of 380 MHz and depression angles of 21°, 25°, and 28°. Figure 3a shows the complete scene with a trihedral reflector in the middle of the image (red rectangle) to analyze the geometric resolution.

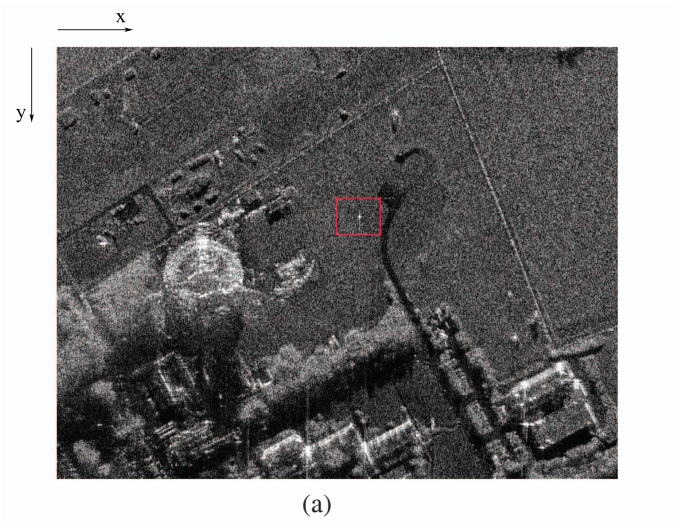

(a)

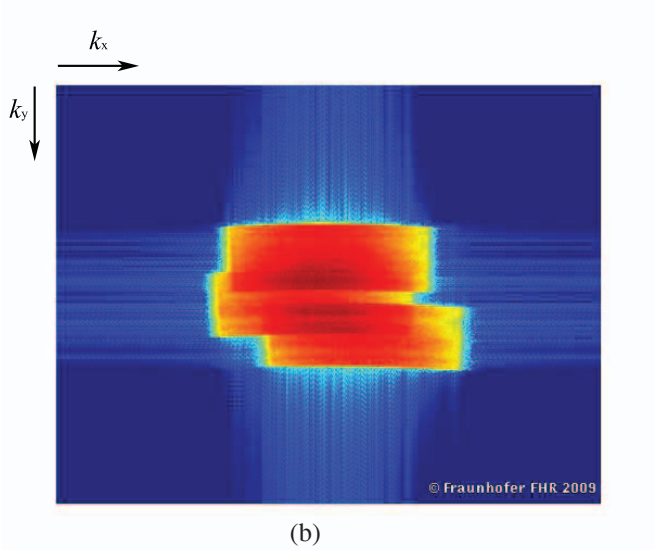

(b)

Fig. 3. (a) Monostatic SAR image with a trihedral (red rectangle) and (b) pure superposition of the ground projected **k**-sets of the three data sets without any processing.

Figure 3b shows the two-dimensional Fourier transform of the scene highlighted by the red rectangle in Fig. 3a superimposed with the corresponding **k**-sets of the other two monostatic data acquisitions. In the final paper the coherent combination of the

three images without **k**-space overlapping will be performed and the geometric resolution improvement will be demonstrated using the response of the corner reflector.

6. ACKNOWLEDGEMENTS

The work reported herein has been funded by German Science Foundation (DFG), grant number EN 731/1-2 and EN 731/2-2, which is gratefully acknowledged. The authors would like to thank the Bundeswehr Technical Center WTD 61 for the performance of the flight trials.

7. REFERENCES

[1] J. Ender, "The meaning of k-space for classical and advanced SAR-techniques," in *PSIP'2001*, Marseilles, France, January 2001.

[2] I. Walterscheid, J. Klare, A. R. Brenner, J. Ender, and O. Loffeld, "Challenges of a bistatic spaceborne/airborne SAR experiment," in *Proc. EUSAR 2006*, Dresden, Germany, May 2006.

[3] C. Prati and F. Rocca, "Improving slant-range resolution with multiple SAR surveys," *IEEE Trans. Aerosp. Electron. Syst.*, vol. 29, no. 1, pp. 135–143, Jan. 1993.

[4] F. Gatelli, A. M. Guamieri, F. Parizzi, P. Pasquali, C. Prati, and F. Rocca, "The wavenumber shift in SAR interferometry," *IEEE Trans. Geosci. Remote Sens.*, vol. 32, no. 4, pp. 855–865, July 1994.

[5] S. Guillaso, A. Reigber, L. Ferro-Famil, and E. Pottier, "Range resolution improvement of airborne SAR images," *IEEE Geosci. Remote Sens. Lett.*, vol. 3, no. 1, pp. 135–139, Jan. 2006.

[6] A. R. Brenner and J. Ender, "Demonstration of advanced reconnaissance techniques with the airborne SAR/GMTI sensor PAMIR," *Proc. Inst. Elect Eng.–Radar Sonar Navig.*, vol. 153, no. 2, pp. 152–162, Apr. 2006.